Journal of Solid State Chemistry 225 (2015) 305–309

Contents lists available at ScienceDirect

Journal of Solid State Chemistry

journal homepage: www.elsevier.com/locate/jssc

Influence of gadolinium content on the tetragonal to cubic phase transition in zirconia-silica binary oxides

Pallavi Suhasinee Behera, S. Vasanthavel, V. Ponnilavan, S. Kannan*

Centre for Nanoscience and Technology, Pondicherry University, Puducherry-605 014, India

ARTICLE INFO

Article history:
Received 19 October 2014
Received in revised form
15 December 2014
Accepted 23 December 2014
Available online 6 January 2015

Keywords:
Zirconia
Silica
Gadolinium
Cubic
Tetragonal
Magnetic

ABSTRACT

The present study reports the effect of gadolinium (Gd^{3+}) in zirconia-silica (ZrO_2-SiO_2) binary oxides. The pure ZrO_2-SiO_2 synthesized at 1100 °C was tetragonal. The addition of Gd^{3+} in the concentration range of 5%–10% resulted in the formation of *t*-ZrO_2, whereas higher contents of Gd^{3+} led to the formation of cubic ZrO_2 (*c*-ZrO_2). The presence of Gd^{3+} also affected the lattice parameters of both *t*-ZrO_2 and *c*-ZrO_2. Magnetic studies confirmed a steady increase in the paramagnetic behaviour with increasing content of Gd^{3+}.

1. Introduction

The utilization of zirconia (ZrO_2) for load bearing orthopaedic biomedical applications is commercially well established over the past three decades [1–3]. Majority of the commercial ZrO_2 are available in the form of its metastable tetragonal polymorph that is generally induced by the yttrium additions in the range of 3–8 wt.%. The addition of yttrium has great potential in stabilizing the tetragonal ZrO_2 (*t*-ZrO_2) at room temperature by preventing its crack propagation that induces its phase transformation to monoclinic ZrO_2 (*m*-ZrO_2) during the cooling process [4]. The prime reason for the formation of metastable *t*-ZrO_2 by yttrium addition is mainly due to the difference in valence between Zr^{4+} and Y^{3+}, causing oxygen vacancies in the crystal lattice of ZrO_2 [5]. The application of metastable *t*-ZrO_2 in clinical practices has been reported with failures due to the concerns of wear and osteolysis around the implant [6]. The clinical failures due to the ageing phenomena at the implant site for considerable time period are also reported [7,8]. During the ageing process, the gradual conversion of *t*-ZrO_2 to *m*-ZrO_2 transformation is found unavoidable and this effect is mainly based on the grain size, yttrium content, residual stresses and specific orientation on the surface. A detailed review presented by Chevalier [9] states that *in vivo* implantation of ZrO_2 after 9 years resulted in about 20% weight fraction of *m*-ZrO_2 and this degradation is expected to be a major cause of strength weakening of the ceramic.

In finding a suitable alternative, the development of metastable *t*-ZrO_2 with an aid of a suitable additive could be a viable option. A report from the previous study states that the addition of 0.5 wt.% silica (SiO_2) to the metastable *t*-ZrO_2 tended to significantly reduce its transformation to *m*-ZrO_2 [10]. The addition of SiO_2 to the ZrO_2 matrix without the presence of yttrium has the ability to form metastable *t*-ZrO_2. However, the concept of stabilization phenomena with the individual presence of either SiO_2 or Y^{3+} in the ZrO_2 matrix is different. The stabilization by Y^{3+} is assisted by the formation of oxygen vacancies, whereas the stabilization by SiO_2 is due to the formation of Si-O-Zr bonds and/or formation of non-bridging oxygen groups (Si-O^-) [11,12]. A few works have been reported on the stabilization phenomena of ZrO_2 by using SiO_2, which are not focused on their biomedical importance [13,14]. The salient features of SiO_2 in biomedical applications are explored well since the discovery of Bioglass by Hench and co-workers [15–17]. Bioglasses are well known for their better mechanical features on comparison with the generally employed Hydroxyapatite [HAP, $Ca_{10}(PO_4)_6(OH)_2$] or β-Tricalcium phosphate [β–TCP, β-$Ca_3(PO_4)_2$]. Moreover, the bioactivity features of bioglass depend on the SiO_2 content, which induces the apatite nucleation by forming silanol (Si-OH) groups on the surface. Hence, the combination of mechanically stable ZrO_2 and bioactive SiO_2 to yield metastable *t*-ZrO_2 is expected be a welcoming prospect for applications in biomedicine.

Further, recent investigations have shown that rare earth element gadolinium (Gd^{3+}) has medical applications as a contrast agent in magnetic resonance imaging (MRI) [18–21]. MRI is a non-invasive

---

* Corresponding author. Tel.: +0091 413 2654973.
E-mail addresses: para_kanna@yahoo.com, skannan.nst@pondiuni.edu.in (S. Kannan).

http://dx.doi.org/10.1016/j.jssc.2014.12.029
0022-4596/

technique used to monitor the performance/structures of internal tissues and organs by generating sectional images. Free Gd^{3+} ion is considered highly toxic and hence it is generally employed by forming complexes with suitable chelating agents that does not hinder its magnetic properties. A detailed review by Telgmann et al., [22] highlighted the importance of Gd^{3+} complexes in medical and environmental applications. A recent investigation has entrusted that Gd^{3+} complexes immobilized in silica particles had the potential to function as MRI contrast agent, with long residence time and non-aggregation in living bodies [23]. The performance of orthopaedic implants during their presence at the implant site for long durations needs a periodical monitoring and hence invasive surgical techniques is not entertained often for observing the implant performance. A potential option could be the use of Gd^{3+} in the implant, to monitor the implant performance through MRI. Thus, the present study aims to develop metastable ZrO_2 with SiO_2 and Gd^{3+} by using sol-gel synthesis. The influence of Gd^{3+} on the structure of ZrO_2 and its effect on magnetic properties were studied.

2. Materials and methods

2.1. Powder synthesis

The Gd^{3+} doped ZrO_2-SiO_2 binary oxides were synthesized by using a sol-gel technique. Gadolinium (III) nitrate hexahydrate [$Gd(NO_3)_3.6H_2O$, Sigma-aldrich, India], zirconium oxychloride octahydrate [$ZrOCl_2 \cdot 8H_2O$, Hi-Media, India] and tetraethyl orthosilicate [$(C_2H_5)_4OSi$, TEOS, Sigma-aldrich, India] were used as precursors. Five concentrations were studied, 5%, 10%, 15%, 20% and 25%. The samples were respectively coded as GZS 5, GZS 10, GZS 15, GZS 20 and GZS 25. Additionally, ZrO_2-SiO_2 sample without the addition of $Gd(NO_3)_3.6H_2O$ was prepared for comparison.

The solution of 1 M $ZrOCl_2 \cdot 8H_2O$ was prepared separately in 200 ml standard measuring flask using millipore water. Separately, $Gd(NO_3)_3.6H_2O$ was dissolved in millipore water, which was added to the $ZrOCl_2 \cdot 8H_2O$ solution. 150 ml of ethanol as a solvent was added to this mixture and the solution mixture was transferred to a 500 ml beaker and placed on a magnetic stirrer (TARSONS, INDIA) at 80 °C and rotation speed of about 300 rpm for 30 min. Then, 1 M TEOS was added to the continuously stirred solution mixtures, followed by the addition of 0.1 M of HNO_3 as a catalyst. The homogeneous solution was slowly stirred for a few hours to yield a precursor gel, which was dried at 120 °C overnight. The dried gel samples were grounded to fine powders. This was followed by heat treatment at different temperatures for 4 h.

2.2. Powder characterization

The powders were analysed by using a high resolution X-ray diffractometer (RIGAKU, ULTIMA IV, JAPAN) with Cu Kα radiation (λ=1.5406 nm) produced at 40 kV and 30 mA to scan the diffraction angles (2θ) between 10 and 70° with a step size of 0.02°. The Raman spectroscopic analysis was employed to determine the vibrational modes of the powders by using back scattering geometry of Confocal Raman microscope (RENISHAW, UNITED KINGDOM). All the samples were excited at a wavelength of 785 nm by using a semiconductor diode laser (0.5% of power) with the data acquiring time of 30 s. Thermal analysis (TG /DTA) was conducted in static air with a thermal analyser (TA INSTRUMENTS, MODEL: Q600 SDT AND Q20 DSC). About 20 mg of powders was used.

2.3. Quantitative analysis by Rietveld refinement

Quantitative analysis was performed by employing Rietveld method using GSAS-EXPGUI software package [24,25]. An average of three scans was recorded for each sample. The standard crystallographic data for the refinement of *t*-ZrO_2, *m*-ZrO_2 and *c*-ZrO_2 were from Howard *et.al.* [26], Smith et al. [27] and Wyckoff [28], respectively. Numerous cycles were run to determine the quantitative analysis, weight fraction and structural parameters of the powders. In the first step of the refinement, all the structural parameters were fixed to the literature values. During the successive refinement cycles, numerous parameters were allowed to vary accordingly to the relative weight amount of the observed phases. The following refinement sequence has been used as a standard for all the structures: scale factor, zero shift, background as Chebyshev polynomial of fifth grade, peak profile, lattice parameters. Fittings were performed using the pseudo-Voigt peak profile functions and a preferred orientation along [001] was taken into account with the Marsh model. The fractional coordinates, isotropic temperature and atomic parameters were employed during the refinement.

2.4. Magnetic measurements

Magnetic hysteresis measurements were carried out by using a vibrating sample magnetometer (VSM, LAKE SHORE 7404) under applied magnetic field at room temperature with a maximum field of 15 k Gauss. The powder samples were wrapped in a Teflon tape and the temperature range was varied from −10 K to 10 K.

3. Results and discussion

3.1. Phase composition

TG-DTA results for selected samples are presented in Fig. 1. All the powders have shown similar weight loss of about 40 wt.% at 500 °C and thereafter the weight loss is negligible. In differential thermograms, two endothermic peaks were witnessed in the region between 80–110 °C and 220–280 °C. The first endothermic region is attributed to the loss of adsorbed water, whereas the second endothermic region is accounted for the evaporation of volatile impurities, such as alkoxides, chlorides and nitrates. Both the observed endothermic peaks could not be accounted for any phase transformation, since XRD patterns of the 300 °C and 500 °C samples (Figs. 2–4) have not indicated the presence of any crystalline phases.

Heat treatment at 600 °C resulted in the emergence of peaks and further heat treatment at 1100 °C has led to the formation of well-defined diffraction peaks that are attributed for ZrO_2. PZS, GZS 5 and GZS 10 are single phase *t*-ZrO_2, whereas GZS 15, GZS 20 and GZS 25 are *c*-ZrO_2. The *t*-ZrO_2 and *c*-ZrO_2 are thermally stable till 1100 °C and heat treatment beyond 1100 °C resulted in their decomposition to *m*-ZrO_2 and zirconium silicate ($ZrSiO_4$).

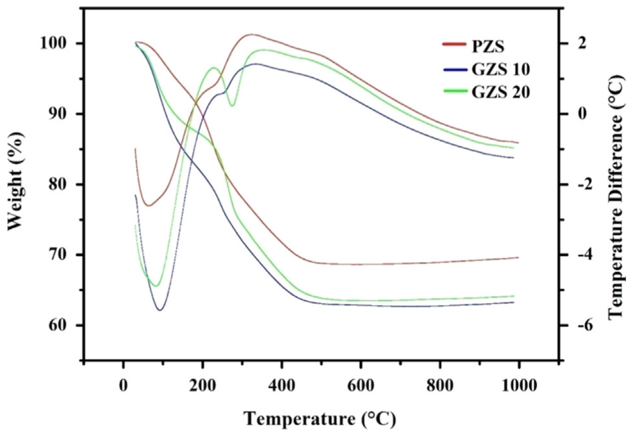

Fig. 1. Thermal behaviours of ZrO_2-SiO_2 and Gd^{3+} doped SiO_2-ZrO_2.